**Earthline Journal of Chemical Sciences**
E-ISSN: 2581-9003; CODEN: EJCSB4
Volume 13, Number 4, November 2026, Pages 475-489
https://doi.org/10.34198/ejcs.13426.33.475489

# Effect of zinc(+2) on some stereoisomers of penicillanic acid – A DFT study

**Lemi Türker**

Department of Chemistry, Middle East Technical University, Üniversiteler, Eskişehir Yolu No: 1, 06800 Çankaya/Ankara, Turkey
e-mail: lturker@gmail.com; lturker@metu.edu.tr

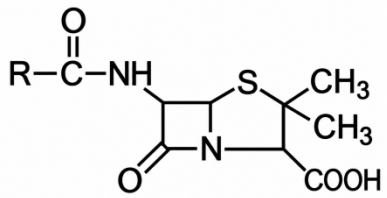
**Abstract**

Presently, some penicilloic acid stereoisomers/tautomers and then their interactions with zinc cation have been investigated within the constraints of density functional theory (DFT) theory at the level of B3LYP/6-31++G(d,p). Various data have been collected. The optimized structures of them have exothermic heats of formation and favorable Gibbs free energy of formation values. They are thermally favored and electronically stable at the standard states. Various structural and quantum chemical data have been collected and discussed, including bond densities and time dependent density functional UV-VIS spectra.

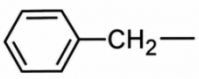
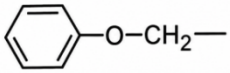
## 1. Introduction

In 1929 Fleming discovered a strain of a mould which inhibits the growth of the staphylococcus [1]. However, the healing properties of green mould were known long before Fleming's discovery to the Russian scientists, Manasein and Polotehnov [1].

All peniccilins share the basic structure of a thiazoldine ring (A) attached to a β-lactam ring (B) that carriers a secondary amine group. The structural integrity of 6-aminopenicillanic acid nucleus is essential to the biological activity of the molecules [2,3]. If the β-lactam ring is enzymatically cleaved, the resulting product penicilloic acid is devoid of antibacterial activity [2]. Later on, a group of researchers at Oxford University isolated a crude substance made up of a few low-molecular substances, which were penicillins (F, G, K, O, V, X). Penicillin G (benzylpenicillin), the most active of these, was suggested for clinical trials in 1941 [3].




penicillins

| Structure of R radical | Name of Penicillin |
|---|---|
|  | Penicillin G<br>Benzylpenicillin |
|  | Penicillin V<br>Phenoxymethylpenicillin |

Received: October 6, 2026; Accepted: November 9, 2026; Published online: November 12, 2026

Keywords and phrases: penicilloic acid, zinc cation, stereoisomer, UV-VIS spectra, DFT calculations.

Copyright © 2026 the Author

Penicillanic acid is the core, bicyclic ring structure, common to all penicillin antibiotics, consisting of a 4-membered β-lactam ring fused with a 5-membered thiazolidine ring (the penam core).

Penicillanic acid and its derivatives are produced when reconstituted penicillins break down in solution from acidity or temperature elevation. Minor determinants of allergy are benzyl penicillin itself and sodium benzyl penicilloate, which can act either as sensitizing agents or on their own elicit an allergic reaction. Both major and minor determinants may be involved in anaphylactic reactions, as well as in urticarial reactions [2,3].

Since then various studies appeared in the literature [4-13] investigating the novel syntheses, reactions, properties and some theoretical aspects of penicillanic acid and its derivatives.

In the present treatment, effect of zinc cation on some stereoisomers/tautomers of penicillanic acid has been considered.

## 2. Method of Calculations

In the present study, all the initial optimizations of the structures leading to energy minima have been achieved first by using MM2 method which is then followed by semi empirical PM3 self consistent fields molecular orbital method [14-16]. Afterwards, the structure optimizations have been achieved within the framework of Hartree-Fock and finally by using density functional theory (DFT) at the level of B3LYP/6-31++G(d,p) [17,18]. Note that the exchange term of B3LYP consists of hybrid Hartree-Fock and local spin density (LSD) exchange functions with Becke's gradient correlation to LSD exchange [19]. The correlation term of B3LYP consists of the Vosko, Wilk, Nusair (VWN3) local correlation functional [20] and Lee, Yang, Parr (LYP) correlation correction functional [21]. In the present study, the normal mode analysis for each structure yielded no imaginary frequencies for the $3N–6$ vibrational degrees of freedom, where $N$ is the number of atoms in the system. This search has indicated that the structure of each molecule considered corresponds to at least a local minimum on the potential energy surface. Furthermore, all the bond lengths have been thoroughly searched in order to find out whether any bond cleavages occurred or not during the geometry optimization process. All these computations were performed by using SPARTAN 06 program [22].

## 3. Results and Discussion

Presently, some tautomers of penicillanic acid (3,3-Dimethyl-7-oxo-4-thia-1-azabicyclo[3,2,0]heptane-2-carboxylic acid) stereoisomers are considered [23]. The considered structures possess two chiral centers which occur at positions 2- and 5- of the skeleton and they are (2S,5R) and (2R,5R). Figure 1 displays numbering of the penicillanic acid skeleton considered and the kind of hetero atoms possessed. The optimized structures of them are depicted in Figure 2. The arrows stand for the direction of calculated dipole moment vectors which are the vectorial sum of the individual bond dipoles, thus location of the heteroatoms greatly affects both the magnitudes and the directions.

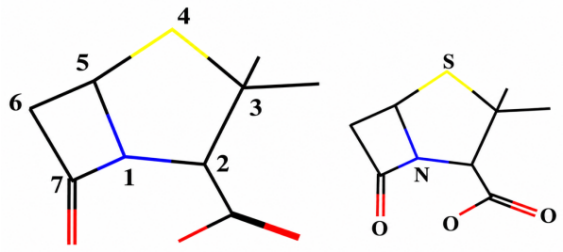



**Figure 1.** Numbering of the penicillanic acid skeleton considered.

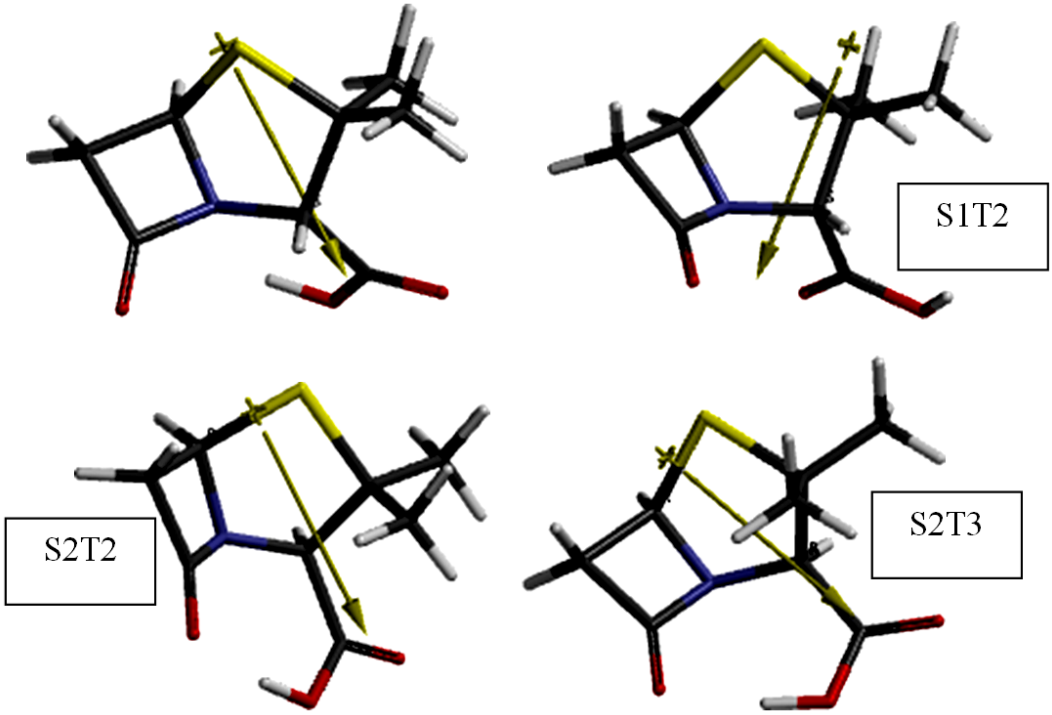



**Figure 2.** Optimized structures of the penicillanic acid species considered.

Some thermo chemical properties of the structures considered are listed in Table 1. The data presented in the table reveal that the standard thermo chemical formation data of all the species considered are exothermic ($H^o$ values) and they are favored according to their $G^o$ (Gibbs free energy of formation) values. The algebraic orders of $H^o$ and $G^o$ values are the same that is S2T2< S2T3< S1T1< S1T2.

**Table 1.** Some thermo chemical properties of the optimized structures of penicillanic acid species considered.

| No. | Species considered | Chiral centers | $H^o$ | $S^o$ (J/mol$^o$) | $G^o$ |
|---|---|---|---|---|---|
| 1 | S1T1 | (2S,5R) | -2599070.992 | 424.79 | -2599197.642 |
| 2 | S1T2 | (2S,5R) | -2599046.325 | 426.68 | -2599173.542 |
| 3 | S2T2 | (2R,5R) | -2599076.028 | 424.82 | -2599202.688 |
| 4 | S2T3 | (2R,5R) | -2599075.581 | 424.50 | -2599202.147 |

Energies in kJ/mol.

As seen in the table the associated chirality of S1T1 and S1T2 are the same (also S2T2 and S2T3 pair wise the same), but the difference is due to conformation of the acid group in space (see Figure 2).

Some energies of the structures considered are included in Table 2, where E, ZPE and $E_C$ stand for the total electronic energy, zero point vibrational energy and the corrected total electronic energy, respectively. According to the data, all the structures are electronically stable. The table indicates that order of the stabilities is S2T2> S2T3> S1T1> S1T2.

**Table 2.** Some energies of the optimized structures of penicillanic acid species considered.

| Species considered | E | ZPE | $E_C$ |
|---|---|---|---|
| S1T1 | -2599573.79 | 495.41 | -2599078.38 |
| S1T2 | -2599548.86 | 494.79 | -2599054.07 |
| S2T2 | -2599578.55 | 495.08 | -2599083.47 |
| S2T3 | -2599578.79 | 495.80 | -2599082.99 |

Energies in kJ/mol.

Figure 3 displays the ESP charges on the atoms of the structures considered. The ESP charges are obtained by the program based on a numerical method that generates charges that reproduce the electrostatic potential field from the entire wavefunction [22]. All the structures possess partially negatively charged sulfur atom. The ESP charges on heteroatoms seem to be quite susceptible to structural variations and it might be related to their electronegativity differences arising from atomic and bonding variations they have in the structures.

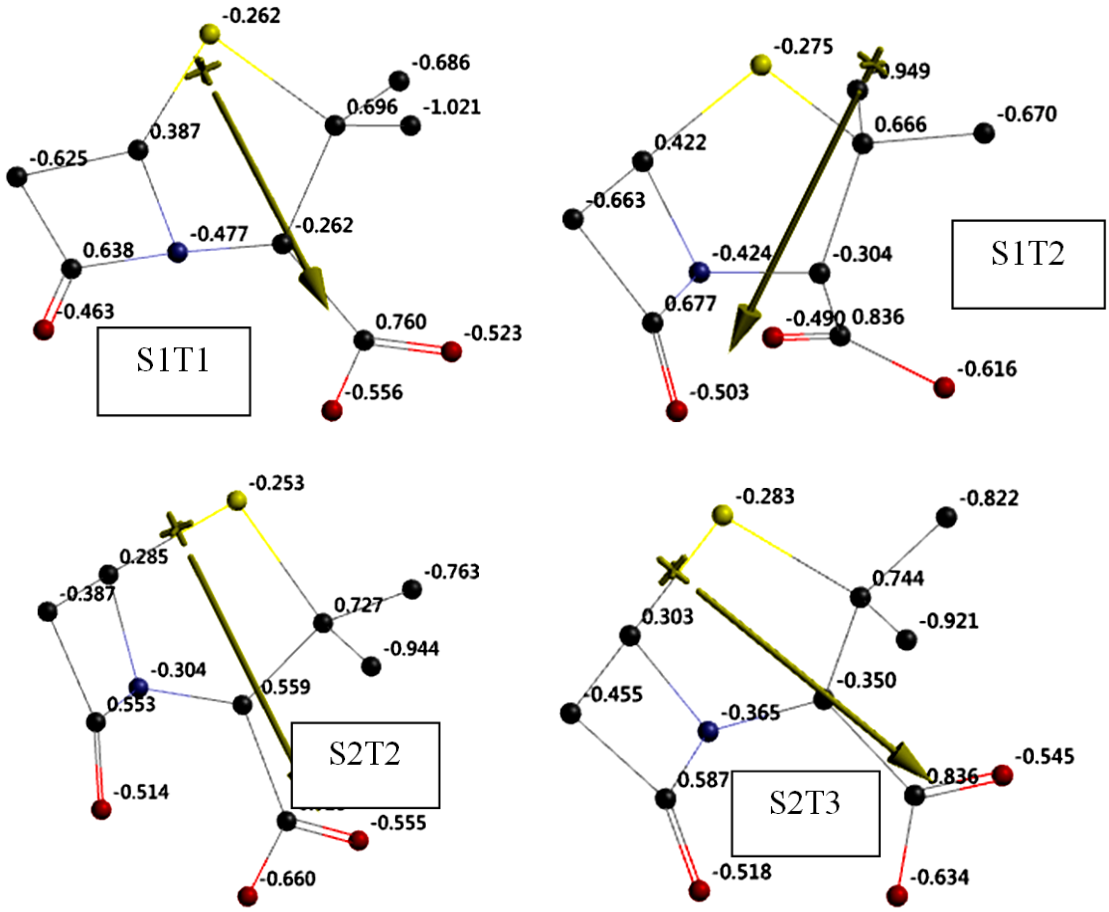



**Figure 3.** ESP charges on atoms of the penicillanic acid species considered.

Figure 4 shows the electrostatic potential maps of the penicillanic acid species (isomers/tautomers) considered. In the presence of zinc cation, all turn into dark blue that no shade differences are observable at all. Note that electro static potential is the energy of interaction of a positive charge with the nuclei and fixed electron distribution of a molecule [22]. In an electrostatic potential map negative potential regions reside on red/reddish and positive ones on blue/bluish parts of the maps.

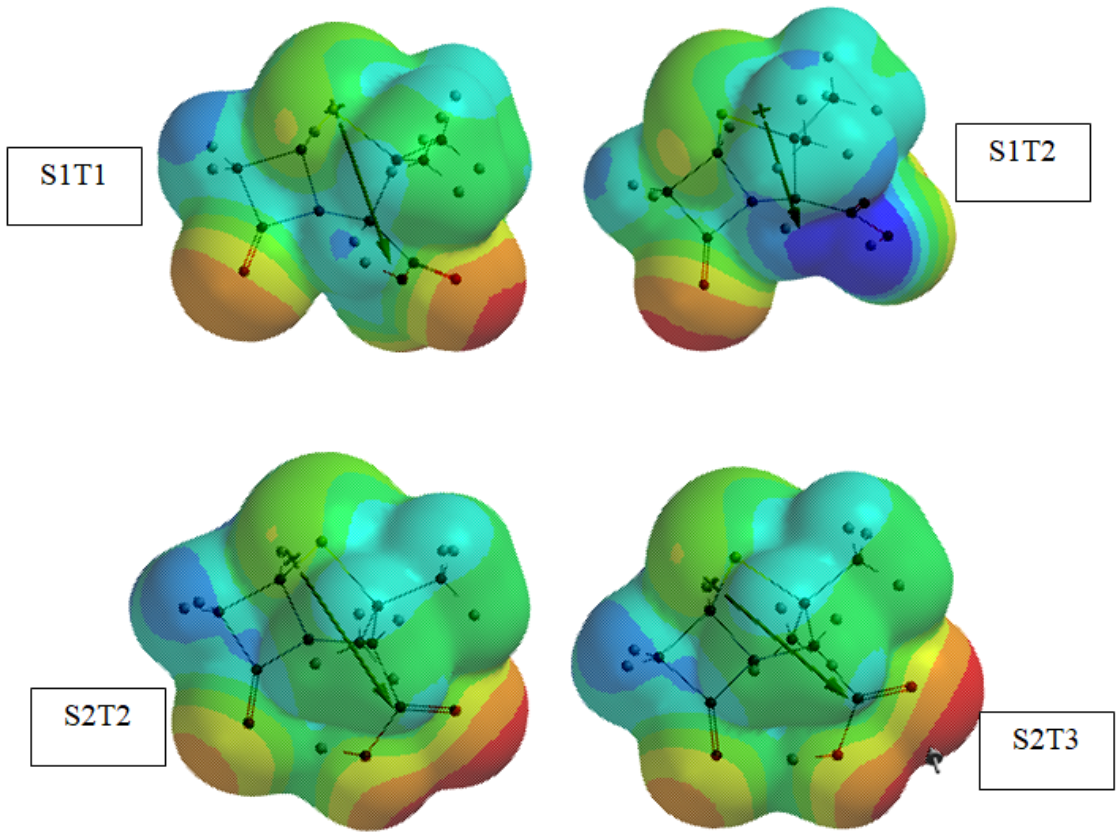
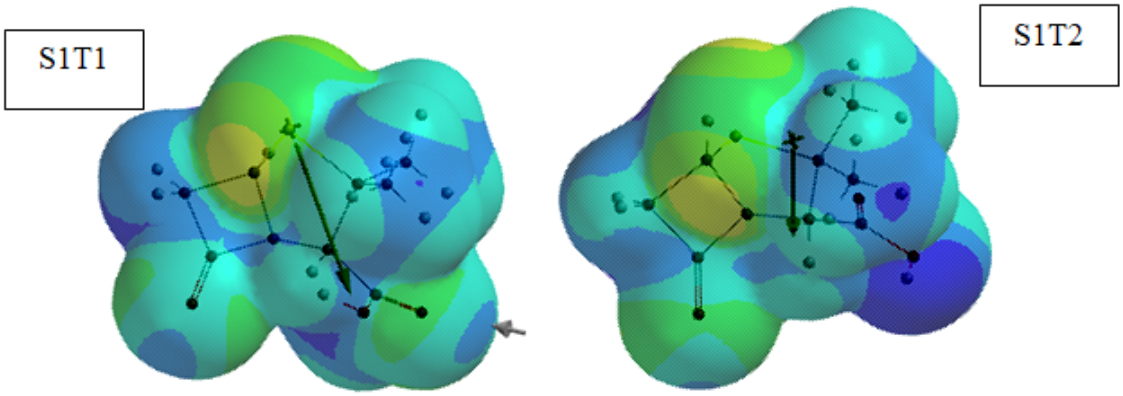



**Figure 4.** Electrostatic potential maps of the penicillanic acid species considered.

Figure 5 displays the local ionization potential maps of the penicillanic acid species considered. The local ionization potential maps of the species where conventionally red/reddish regions (if any exists) on the density surface indicate areas from which electron removal is relatively easy, meaning that they are subject to electrophilic attack. Note that the local ionization potential map is a graph of the value of the local ionization potential on an isodensity surface corresponding to a van der Waals surface [22]. The existing colored patches are indicative of existence of rather rough potential surfaces.

In the presence of zinc cation, all the local ionization potential maps of the penicillanic acid species turn into dark blue.



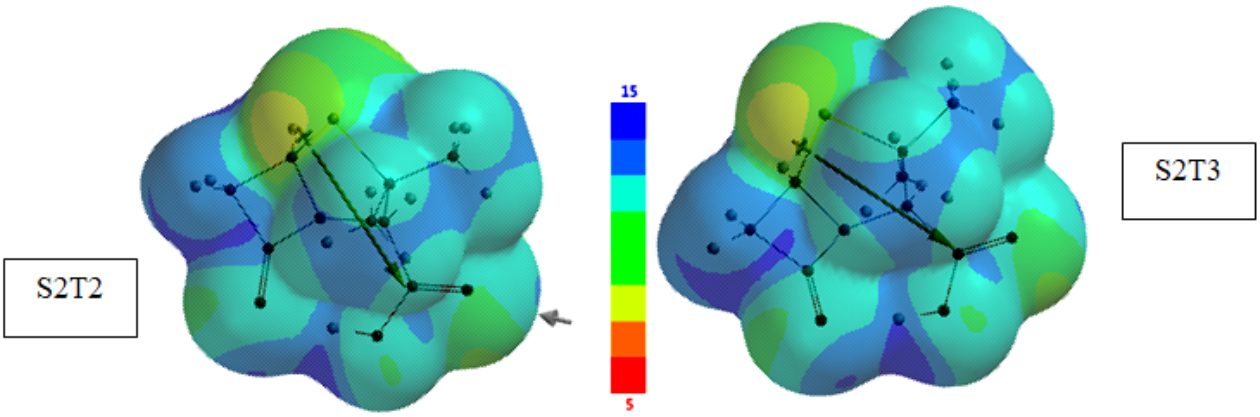



**Figure 5.** Local ionization potential maps of the penicillanic acid species considered.

Figure 6 shows some of the molecular orbital energy levels of the penicillanic acid structures considered. It is note worthy that the density of inner lying molecular orbitals are related to the thermal stability of a molecule.

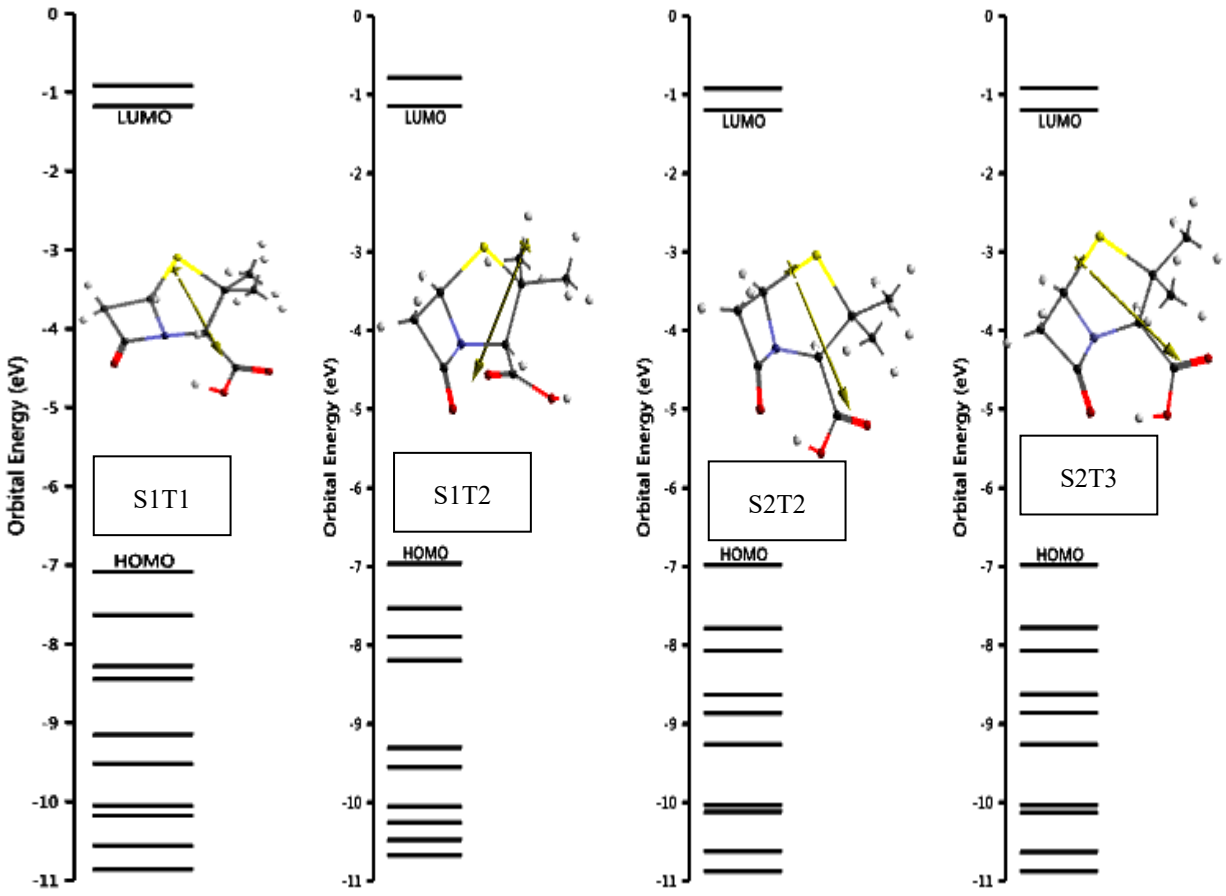



**Figure 6.** Some of molecular orbital energy levels of the penicillanic acid species considered.

Table 3 includes the HOMO, LUMO energies and interfrontier molecular orbital (FMO) energy gap values, $\Delta\varepsilon$ ($\Delta\varepsilon = \varepsilon_{LUMO}-\varepsilon_{HOMO}$) of the structures presented in Figure 2. The algebraic orders of the HOMO and LUMO energies are S1T1< S2T3< S2T2< S1T2 and S2T2< S2T3< S1T1< S1T2, respectively. Thus, the $\Delta\varepsilon$ values

follow the order of S1T1> S1T2> S2T3> S2T2. The structural changes greatly affect both the frontier molecular orbital energies.

**Table 3.** The HOMO, LUMO energies and Δε values of the optimized species considered.

| Species considered | HOMO | LUMO | Δε |
|---|---|---|---|
| S1T1 | -683.21 | -113.17 | 570.04 |
| S1T2 | -671.91 | -110.81 | 561.1 |
| S2T2 | -673.59 | -115.52 | 558.07 |
| S2T3 | -673.93 | -115.20 | 558.73 |

Energies in kJ/mol.

Figure 7 shows the optimized structures of the penicillanic acid+ zinc species (Composites) considered.

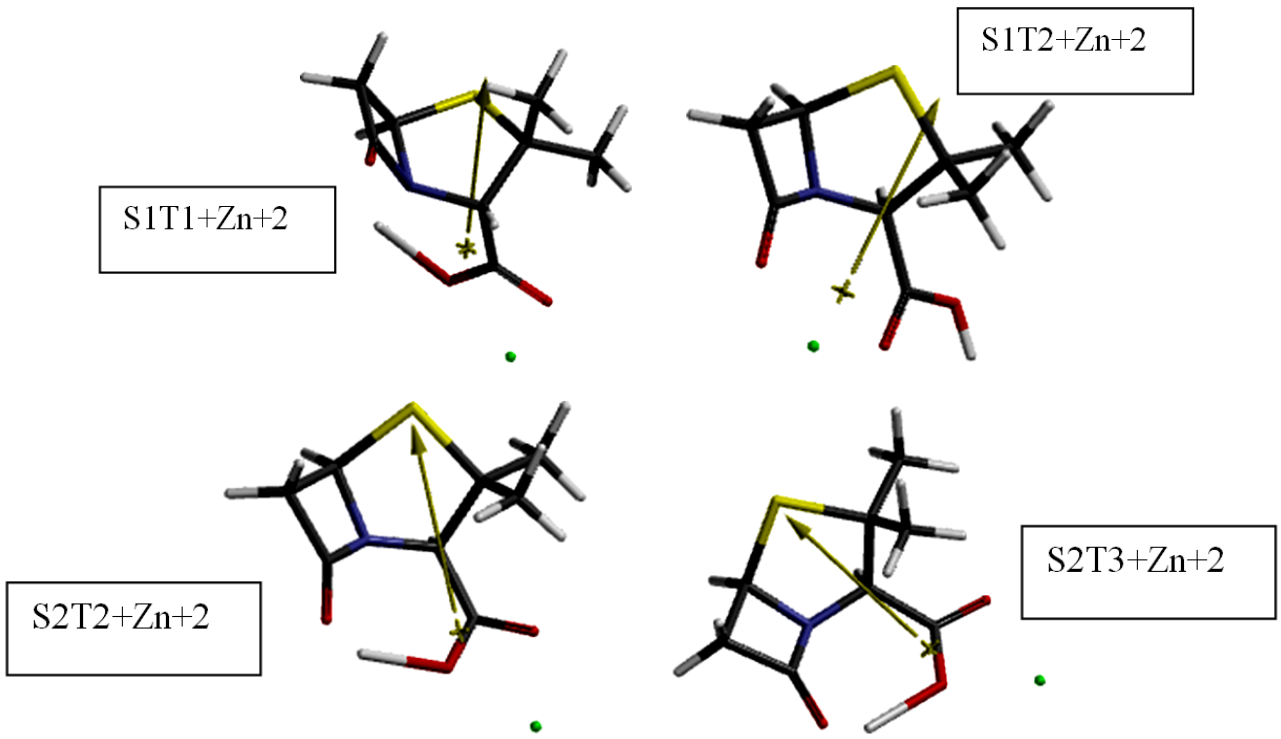



**Figure 7.** Optimized structures of the penicillanic acid+ zinc species considered.

Table 4 tabulates some thermo chemical properties of the Zn(+2) containing structures (Composites) considered and displayed in Figure 7. The data presented in the Table 4 reveal that the standard thermo chemical formation data of all the species considered are exothermic (Hº values) and they are favored according to their Gº (Gibbs free energy of formation) values. The algebraic orders of Hº and Gº values are the same namely; S1T2+Zn+2< S2T2+Zn+2< S2T3+Zn+2< S1T1+Zn+2.

**Table 4.** Some thermo chemical properties of the Zn(+2) containing structures considered.

| No. | Species considered | Chiral centers | Hº | Sº (J/molº) | Gº |
|---|---|---|---|---|---|
| 1' | S1T1+Zn+2 | (2S,5R) | -7268447.328 | 458.45 | -7268584.040 |
| 2' | S1T2+Zn+2 | (2R,5R) | -7268537.148 | 451.20 | -7268671.680 |
| 3' | S2T2+Zn+2 | (2R,5R) | -7268460.167 | 456.51 | -7268596.301 |
| 4' | S2T3+Zn+2 | (2R,5R) | -7268459.983 | 455.26 | -7268595.723 |

Energies in kJ/mol.

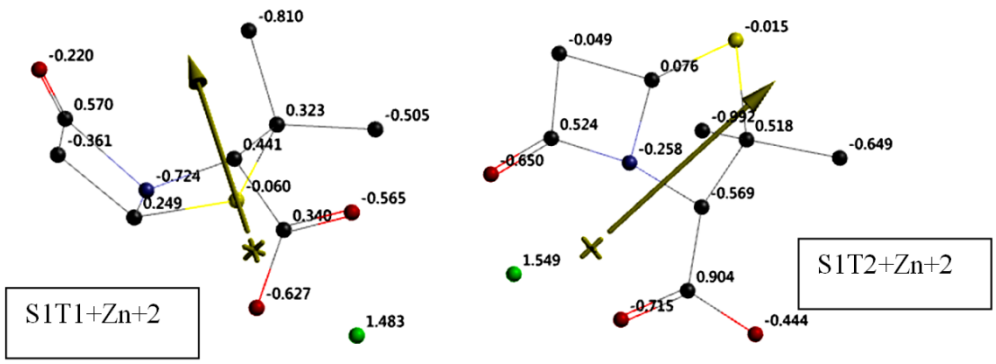
Table 5 list some energies of the Zn(+2) containing structures considered. The stability order appears to be S1T2+Zn+2> S2T2+Zn+2> S2T3+Zn+2> S1T1+Zn+2.

**Table 5.** Some energies of the Zn(+2) containing structures considered.

| Species considered | Chiral centers | E | ZPE | $E_C$ |
|---|---|---|---|---|
| S1T1+Zn+2 | (2S,5R) | -7268911.04 | 495.68 | -7268415.36 |
| S1T2+Zn+2 | (2R,5R) | -7269003.15 | 498.56 | -7268504.59 |
| S2T2+Zn+2 | (2R,5R) | -7268925.95 | 498.10 | -7268427.85 |
| S2T3+Zn+2 | (2R,5R) | -7268926.13 | 498.57 | -7268427.56 |

Energies in kJ/mol.

Figure 8 displays the ESP charges on atoms of the penicillanic acid+ zinc species considered. In these composite structures it is note worthy that the zinc cation is no longer possesses the initial charge of +2 but always has a partial positive charge less than that which is indicative of some of electron transfer from organic moiety to the zinc cation.



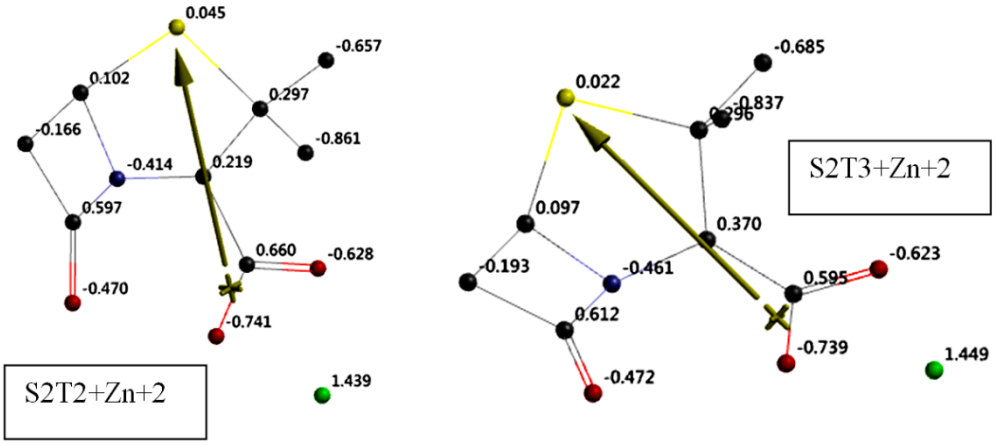



**Figure 8.** The ESP charges on atoms of the penicillanic acid+ zinc species considered.

Figure 9 shows some of molecular orbital energy levels of the penicillanic acid+ zinc species considered. Table 6 contains the HOMO, LUMO energies and Δε (Δε = $\varepsilon_{LUMO}$-$\varepsilon_{HOMO}$) values of the optimized species considered.

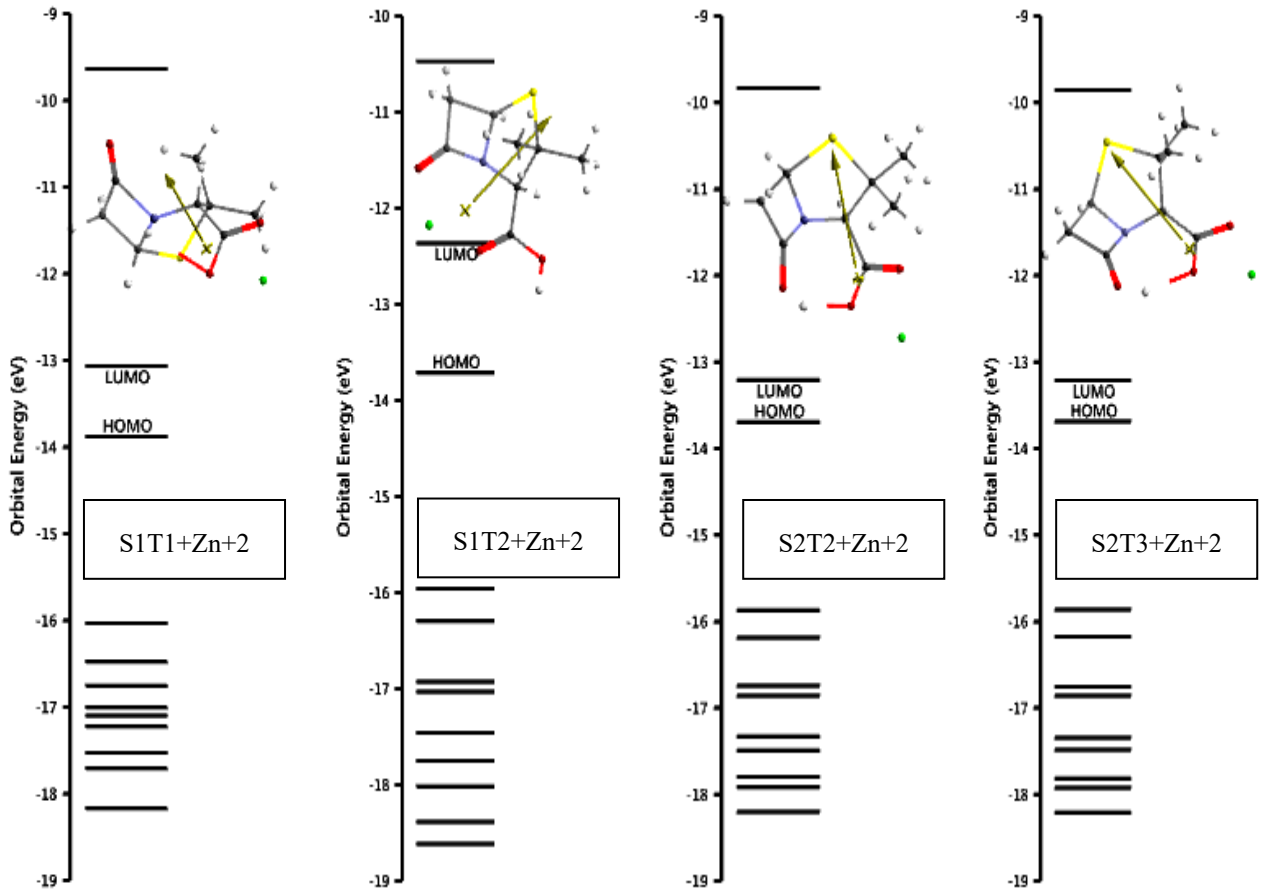



**Figure 9.** Some of molecular orbital energy levels of the penicillanic acid+ zinc species considered.

**Table 6.** The HOMO, LUMO energies and Δε values of the optimized species considered.

| No. | Species | HOMO | LUMO | Δε |
|---|---|---|---|---|
| 1 | S1T1 | -683.21 | -113.17 | -570.04 |
| 1' | S1T1+Zn+2 | -1338.95 | -1260.70 | -78.25 |
| 2 | S1T2 | -671.91 | -110.81 | -561.10 |
| 2' | S1T2+Zn+2 | -1322.92 | -1192.78 | -130.14 |
| 3 | S2T2 | -673.59 | -115.52 | -558.07 |
| 3' | S2T2+Zn+2 | -1321.20 | -1274.38 | -46.82 |
| 4 | S2T3 | -673.93 | -115.20 | -558.73 |
| 4' | S2T3+Zn+2 | -1320.61 | -1274.88 | -45.73 |

Energies in kJ/mol.

The algebraic orders of the HOMO and LUMO energies of the zinc composites are 1'<2'<3'<4' and 4'<3'<1'<2', respectively. Consequently, the order of Δε values happens as 2'<1'<3'<4'. The cation substantially lowers both the HOMO and LUMO energies as compared to the respective energies of the parent compounds. The frontier molecular orbital energy gap values (Δε values) are lowered substantially too.

The bond density maps of the penicillanic acid+ zinc species considered are displayed in Figure 10. The bond density contains fewer electrons in total and demarks atomic connectivity. Figure 10 reveals that in all the cases there exists an interaction between the organic moiety (penicillanic acid) and the zinc cation in different degrees The interaction is at the site of C=O, moiety and acid COH part in S1T1+Zn+2; C=O groups in S1T2+Zn+2 and between the acid COH part and zinc cation in S2T2+Zn+2 and S2T3+Zn+2 composites. Note that in the composites considered the zinc cation possesses less positive partial charge than the initial charge of the zinc cation. For the charges of penicillanic acid species and their respective composites see Figures 3 and 8.

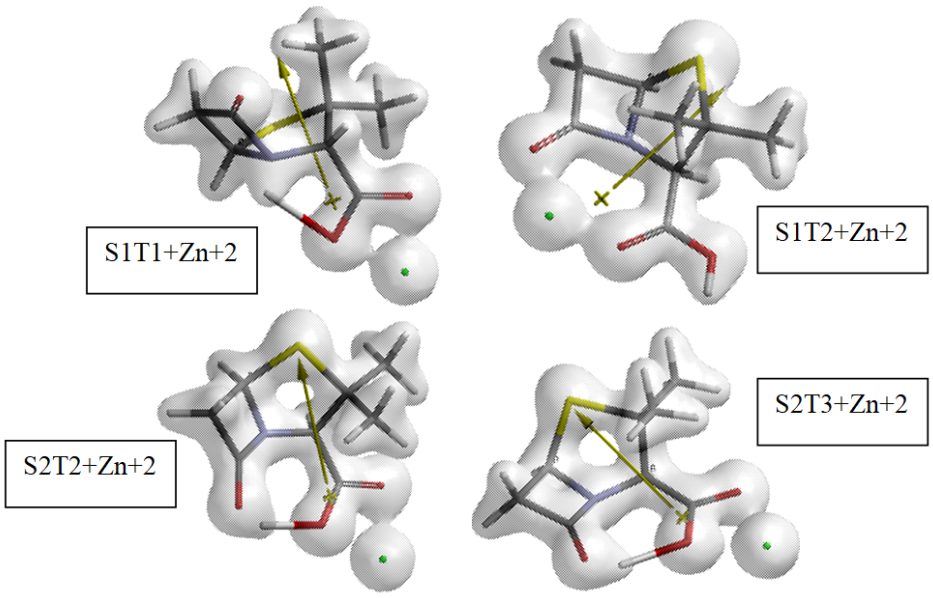



**Figure 10.** Bond density maps of the penicillanic acid+ zinc species considered.

The UV-VIS spectrums of penicillanic acid species (stereo isomers/tautomers) are confined in to UV region of the spectrum. However, their zinc composites of the present concern have the spectra presented in Figure 11. The spectra of them spreads over UV-VIS region. S1T2+Zn+2 spectrum exhibits some hypsochromic shift compared to S1T1+Zn+2 case whereas S2T2+Zn+2 and S2T3+Zn+2 cases have some bathochromic shift as compared to S1T1+Zn+2 and S1T2+Zn+2 spectrums. Note that S1T2+Zn+2 spectra has some shoulders which are not well appeared. The zinc cation, hydrogen bonding tendency as well as stereo isomeric differences between those isomers affect the electron distribution of conjugative paths responsible for the spectra are to be blamed for the observed changes of the calculated spectra.

It is to be said that the calculated intensities of the peaks are related to magnitudes of the transition moments between the orbitals involved which vary from isomer to isomer [24,25].

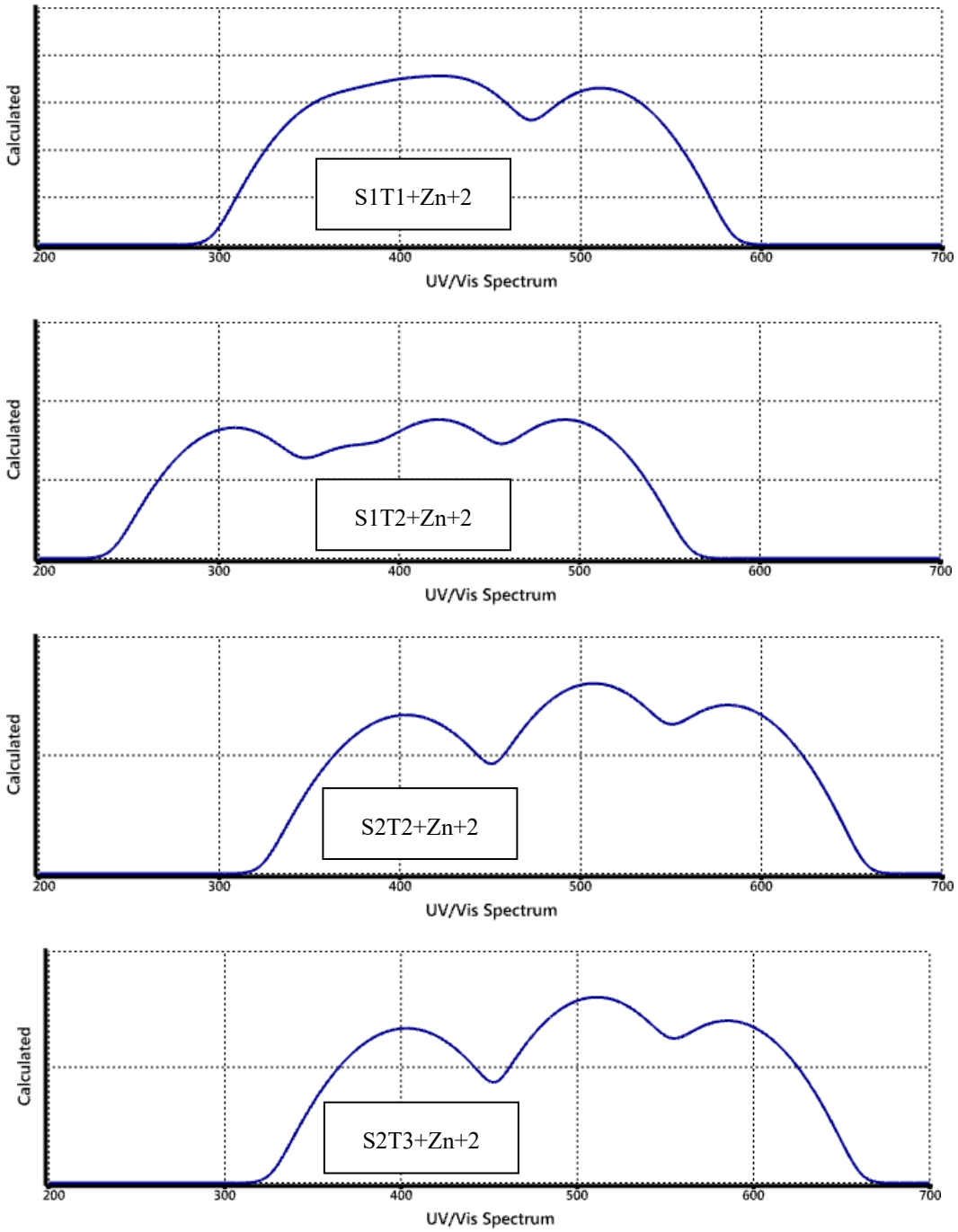



**Figure 11.** UV-VIS spectrums of the penicillanic acid+ zinc species considered.

Table 7 lists the $\lambda_{max}$ values and intensities of the peaks of spectrums of the species of interest.

**Table 7.** The $\lambda_{max}$ (nm) values and intensities of the peaks of the spectrums of species of interest

| Species | $\lambda_{max}$ (nm) |
|---|---|
| S1T1+Zn+2 | 367.87 (0.005), 400.35 (0.011), 400.24 (0.015), 510.74 (0.009) |
| S1T2+Zn+2 | 398.59 (0.002), 421.95 (0.003), 591.77 (0.003) |
| S2T2+Zn+2 | 392.96 (0.002), 405.62 (0.007), 507.24 (0.066), 581.61 (0.018) |
| S2T3+Zn+2 | 396.33 (0.033), 405.39 (0.006), 510.99 (0.064), 585.17 (0.015) |

Intensities are in parenthesis

The effect of the zinc cation on LUMO maps of the penicillanic acid species is seen clearly by comparing the respective Figures 12 and 13. A LUMO map displays the absolute value of the LUMO on the electron density surface. The blue color (if any exists) stands for the maximum value of the LUMO and the red colored region, associates with the minimum value. It is to be noted that the LUMO and NEXTLUMO (LUMO+1) are the major orbitals directing the molecule towards the attack of nucleophiles [22,26]. Positions where the greatest LUMO coefficient exists is the most vulnerable site in nucleophilic reactions. Note that the presence of the zinc cation veils all the shade differences of the LUMO maps of the penicillanic acid species by covering them in dark color.

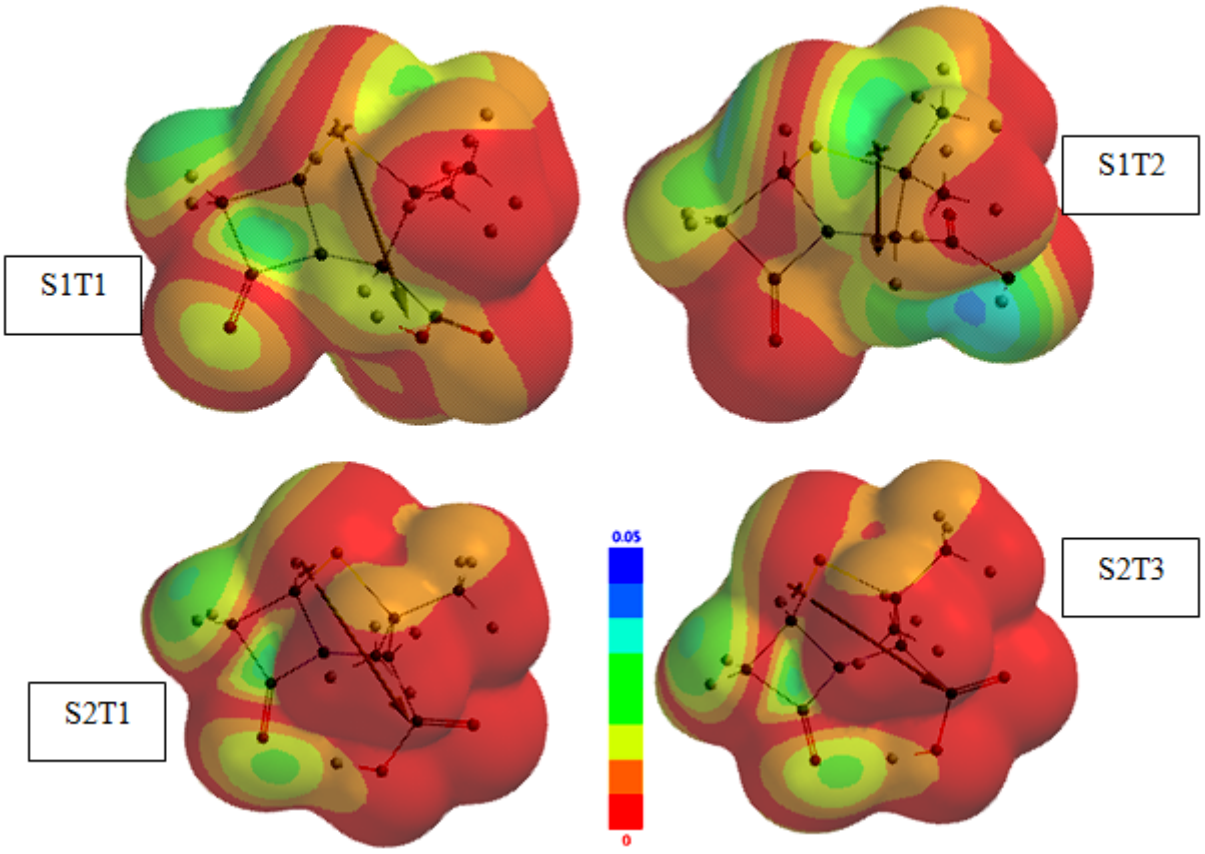



**Figure 12.** The LUMO maps of the penicillanic acid species considered.

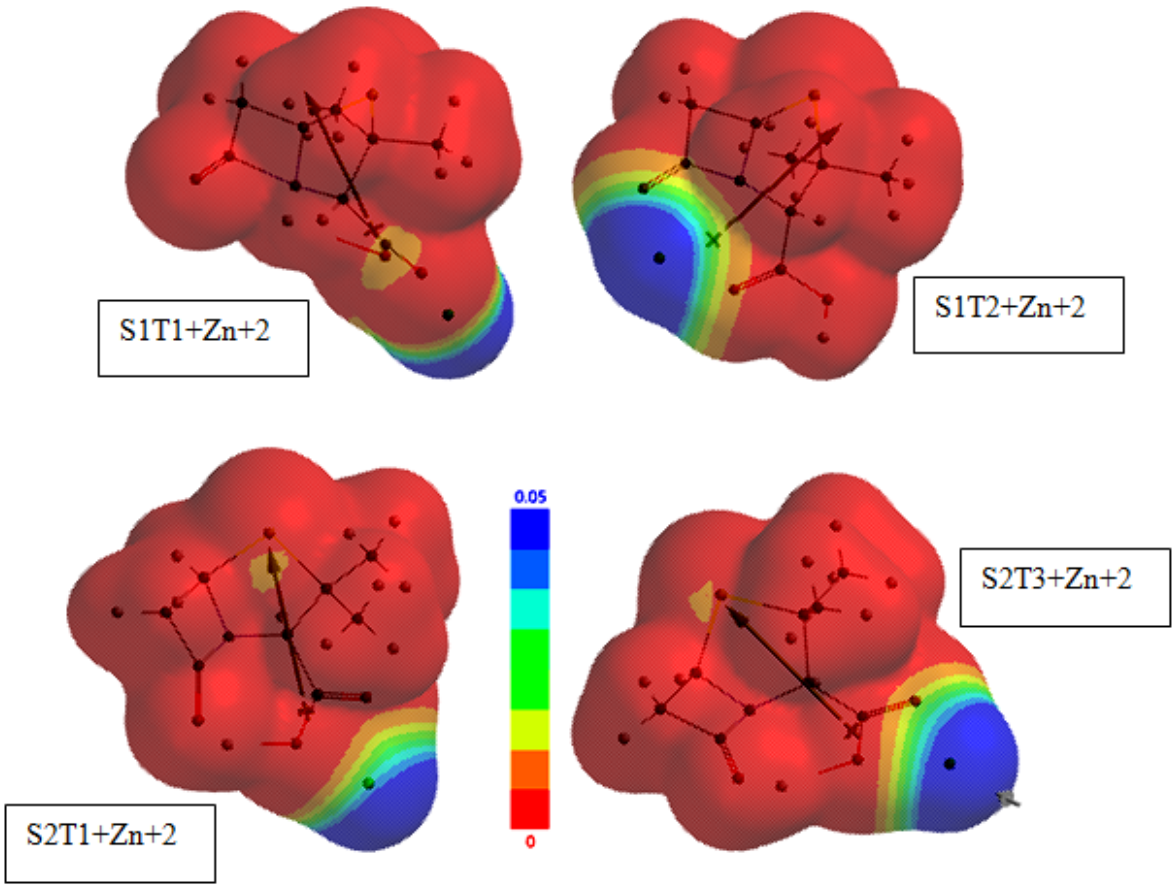



**Figure 13.** The LUMO maps of the penicillanic acid+Zn+2 species considered.

Table 8 shows some properties of the species concerned. The data in the table shows that the cation drastically increases the dipole moment values although its effect on the polarizability values is minute. Note that the polarizability values of the zinc composites are almost constant (like log P values). Their Cv values also vary in a small range. The presence of the cation buffers variation of all those properties.

**Table 8.** Some properties of the species concerned.

| No. | Species | Eaq (kJ/mol) | Dipole (debye) | Polarizability | Log P | Cv (J/mol$^o$) |
|---|---|---|---|---|---|---|
| 1 | S1T1 | -2599609.04 | 5.02 | 54.99 | 0.10 | 150.63 |
| 1' | S1T1+Zn+2 | - | 17.19 | 56.76 | - | 163.92 |
| 2 | S1T2 | -2599609.03 | 4.11 | 55.06 | 0.10 | 151.15 |
| 2' | S1T2+Zn+2 | - | 17.19 | 56.76 | - | 163.92 |
| 3 | S2T2 | -2599725.63 | 5.16 | 54.93 | 0.10 | 149.07 |
| 3' | S2T2+Zn+2 | - | 15.46 | 56.75 | - | 162.14 |
| 4 | S2T3 | -2599726.07 | 5.16 | 54.93 | 0.10 | 148.81 |
| 4' | S2T3+Zn+2 | - | 15.59 | 56.75 | - | 161.96 |

Polarizabilities in $10^{-30}$ $m^3$ units.

## 4. Conclusion

The present study considers interaction of penicillanic acid and zinc cation and leading to penicillanic acid $+Zn^{+2}$ composite and has been subjected to DFT treatment at the level of B3LYP/6-31++G(d,p). The species of interest have exothermic heats of formation and favorable Gibbs free energy of formation values and are thermally favored and electronically stable at the standard states.

The bond density maps reveal that in all the cases, there exists an interaction between the organic moiety (penicillanic acid) and the zinc cation in different degrees. In all the composites the zinc cation possesses less positive partial charge than the initial charge of the zinc cation which is indicative of some of electron transfer from the organic moiety to the zinc cation has occurred.

Most of the properties of penicillanic acid stereoisomers/tautomers which are presently considered, including molecular orbital energies and UV-VIS spectrums are affected by the zinc cation. Both the HOMO and LUMO energies are lowered as compared to the respective energies of the parent compounds. The frontier molecular orbital energy gap values (Δε values) are lowered substantially too.

## References

[1] Malentyeva, G., & Antonova, L. (1988). *Pharmaceutical chemistry* (Eng. ed.). Mir Publishers.

[2] Javetz, E. (1984). Penicillins and cephalosporins. In B. G. Katzung (Ed.), *Basic and clinical pharmacology*. Lange Medical Publications.

[3] Vardanyan, R. (2006). *Synthesis of essential drugs*. Elsevier. https://doi.org/10.1016/B978-0-444-52166-8.X5000-6

[4] Neu, H. C. (1976). Mecillinam, a novel penicillanic acid derivative with unusual activity against gram-negative bacteria. *Antimicrobial Agents and Chemotherapy, 9*(5), 793–798.

[5] Stoodley, R. J. (1975). Rearrangements of penicillanic acid derivatives. *Tetrahedron, 31*(19), 2321–2345. https://doi.org/10.1016/0040-4020(75)80235-3

[6] Demirci, S., Demirbas, A., Ulker, S., Alpay-Karaoglu, S., & Demirbas, N. (2014). Synthesis of some heterofunctionalized penicillanic acid derivatives and investigation of their biological activities. *Archiv der Pharmazie, 347*(3), 200–220. https://doi.org/10.1002/ardp.201300280

[7] Chen, X., Liu, J., Fan, J., Bu, Y., Wang, Q., Yan, H., Yu, C., & Lin, Q. (2026). Self-assembly of alginate-grafted penicillanic acid derivatives into antibacterial micelles for controlled drug delivery. *ACS Omega, 11*(13), 20302–20319. https://doi.org/10.1021/acsomega.5c10841

[8] Halipçi-Topsakal, H. N. (2026). Design of novel penicillanic acid derivatives targeting resistant bacterial pathogens and bacterial extracellular vesicles. *Proceedings of the 2nd Extracellular Vesicles Conference* (*TURSEV-26*), Ankara, Türkiye, 4–8 June, 4–5.

[9] Yousif, Q. A., Bedair, M. A., Abuelela, A. M., Al-Odail, F., Ansari, A., & Fadel, Z. (2025). Theoretical and experimental aspects of novel penicillanic acid compounds as corrosion inhibitors in acidic solutions. *Materials Today Communications, 47*, Article 113199. https://doi.org/10.1016/j.mtcomm.2025.113199

[10] Shukla, A., Khan, E., Srivastava, A., Tandon, P., & Sinha, K. (2016). A computational study on molecular structure, multiple interactions, chemical reactivity and molecular docking studies on 6[D (−) α-amino-phenyl-acetamido] penicillanic acid (ampicillin). *Molecular Simulation, 42*(11), 863–873. https://doi.org/10.1080/08927022.2015.1089996

[11] Bou, G., Santillana, E., Sheri, A., Beceiro, A., Sampson, J. M., Kalp, M., Bethel, C. R., Distler, A. M., Drawz, S. M., Pagadala, S. R. R., & Van Den Akker, F. (2010). Design, synthesis, and crystal structures of 6-alkylidene-2′-substituted penicillanic acid sulfones as potent inhibitors of Acinetobacter baumannii OXA-24 carbapenemase. *Journal of the American Chemical Society, 132*(38), 13320–13331. https://doi.org/10.1021/ja104840m

[12] Basoglu, S., Ulker, S., Alpay-Karaoglu, S., & Demirbas, N. (2014). Microwave-assisted synthesis of some hybrid molecules containing penicillanic acid or cephalosporanic acid moieties and investigation of their biological activities. *Medicinal Chemistry Research, 23*(7), 3128–3143. https://doi.org/10.1007/s00044-013-0898-4

[13] Papp-Wallace, K. M., Bethel, C. R., Gootz, T. D., Shang, W., Stroh, J., Lau, W., McLeod, D., Price, L., Marfat, A., Distler, A., Drawz, S. M., Chen, H., Harry, E., Nottingham, M., Carey, P. R., Buynak, J. D., & Bonomo, R. A. (2012). Inactivation of a class A and a class C β-lactamase by 6β-(hydroxymethyl)penicillanic acid sulfone. *Biochemical Pharmacology, 83*(4), 462–471. https://doi.org/10.1016/j.bcp.2011.11.015

[14] Stewart, J. J. P. (1989). Optimization of parameters for semi-empirical methods I. *Journal of Computational Chemistry, 10*(2), 209–220. https://doi.org/10.1002/jcc.540100208

[15] Stewart, J. J. P. (1989). Optimization of parameters for semi-empirical methods II. *Journal of Computational Chemistry, 10*(2), 221–264. https://doi.org/10.1002/jcc.540100209

[16] Leach, A. R. (1997). *Molecular modeling*. Longman.

[17] Kohn, W., & Sham, L. J. (1965). Self-consistent equations including exchange and correlation effects. *Physical Review, 140*(4A), A1133–A1138. https://doi.org/10.1103/PhysRev.140.A1133

[18] Parr, R. G., & Yang, W. (1989). *Density-functional theory of atoms and molecules*. Oxford University Press.

[19] Becke, A. D. (1988). Density-functional exchange-energy approximation with correct asymptotic behavior. *Physical Review A, 38*(6), 3098–3100. https://doi.org/10.1103/PhysRevA.38.3098

[20] Vosko, S. H., Wilk, L., & Nusair, M. (1980). Accurate spin-dependent electron liquid correlation energies for local spin density calculations: A critical analysis. *Canadian Journal of Physics, 58*(8), 1200–1211. https://doi.org/10.1139/p80-159

[21] Lee, C., Yang, W., & Parr, R. G. (1988). Development of the Colle-Salvetti correlation energy formula into a functional of the electron density. *Physical Review B, 37*(2), 785–789. https://doi.org/10.1103/PhysRevB.37.785

[22] Spartan 06. (2006). *Wavefunction Inc*.

[23] Windholtz, M., Budavari, S., Blumetti, R. F., & Otterbein, E. S. (Eds.). (1983). *The Merck index* (10th ed.). Merck & Co.

[24] Anslyn, E. V., & Dougherty, D. A. (2006). *Modern physical organic chemistry*. University Science Books.

[25] Turro, N. J. (1991). *Modern molecular photochemistry*. University Science Books.

[26] TRİDENT. (2006). *Molecular modeling for medicinal chemists*. Wavefunction Inc.

This is an open access article distributed under the terms of the Creative Commons Attribution License (http://creativecommons.org/licenses/by/4.0/), which permits unrestricted, use, distribution and reproduction in any medium, or format for any purpose, even commercially provided the work is properly cited.